

# Reward Design for Driver Repositioning Using Multi-Agent Reinforcement Learning

Zhenyu Shou<sup>a</sup>, Xuan Di<sup>a,b,\*</sup>

<sup>a</sup>*Department of Civil Engineering and Engineering Mechanics, Columbia University*

<sup>b</sup>*Data Science Institute, Columbia University*

---

## Abstract

A large portion of the passenger requests is reportedly unserved, partially due to vacant for-hire drivers' cruising behavior during the passenger seeking process. This paper aims to model the multi-driver repositioning task through a mean field multi-agent reinforcement learning (MARL) approach. Noticing that the direct application of MARL to the multi-driver system under a given reward mechanism will very likely yield a suboptimal equilibrium due to the selfishness of drivers, this study proposes a reward design scheme with which a more desired equilibrium can be reached. To effectively solve the bilevel optimization problem with upper level as the reward design and the lower level as a multi-agent system (MAS), a Bayesian optimization algorithm is adopted to speed up the learning process. We then use a synthetic dataset to test the proposed model. The results show that the weighted average of order response rate and overall service charge can be improved by 4% using a simple platform service charge, compared with that of no reward design.

**Keywords:** Mean Field Multi-Agent Reinforcement Learning, Reward Design, Bayesian Optimization

---

## 1. Introduction

The emergence of transportation network companies (TNCs) or e-hailing platforms (such as Didi and Uber) has revolutionized the traditional taxi market and provided commuters a flexible-route door-to-door mobility service. Nonetheless, it is reported that a large portion of the passenger requests remain unserved because of the imbalance between demand (i.e., passenger requests) and supply (i.e., available drivers) (Lin et al., 2018), resulting in long cruising trips for taxi drivers to find the next passenger (Powell et al., 2011). Such cruising behavior has negative impact on urban economy by not only decreasing drivers' income but also generating additional vehicle miles traveled. Thus, repositioning available drivers to potential locations with near-future high demand, i.e., to balance supply and demand, becomes the key challenge faced by the taxi and for-hire market, including e-hailing platforms. Leveraging cutting edge machine learning techniques, this paper aims to improve the efficiency of the taxi and for-hire market.

The essence of the repositioning task is to provide recommendations to idle drivers on where to find the next passenger. Some recommender systems have been proposed for drivers (Ge et al., 2010; Hwang et al., 2015; Yuan et al., 2011; Qu et al., 2014). These studies extracted useful aggregated statistical quantities such as taxi demand and travel time from historical data and recommended a next cruising location (Ge et al., 2010), a sequence of potential pickup points (Hwang et al., 2015), a driving route (Qu et al., 2014), or a route and a location (Yuan et al., 2011).

Although the aforementioned studies provide effective recommendations of the next cruising route or location to drivers at the immediate next step, they are nearsighted and fall short of capturing the future long-run payoffs. To capture the effect of future rewards on the recommendation at the immediate next step, various Markov decision process (MDP) based approaches have been proposed to model idle drivers' passenger searching process (Rong et al., 2016; Zhou et al., 2018; Verma et al., 2017; Gao et al., 2018; Yu et al., 2019; Shou et al., 2020). In an MDP with a single agent, a driver is the agent who makes decisions

---

\*Corresponding author. Tel.: +1 212 853 0435;

Email address: sharon.di@columbia.edu (Xuan Di)

of where to go next. The dynamic environment is determined by the stochastic passenger requests and all other traffic information including the road network, distribution of drivers, and traffic conditions. Once the agent makes an action in a state, the agent then transits into a new state and receives an immediate reward by following the dynamics of the environment. The agent aims to derive an optimal policy which maximizes her expected cumulative reward. When the dynamic environment is known to the agent, dynamic programming or value iteration can be used to solve the MDP and derive an optimal policy. When the dynamic environment is unknown to the agent, the agent needs to interact with the environment by the trial and error process and gradually learns an optimal policy by some reinforcement learning (RL) algorithms such as Q-learning and temporal difference learning (Sutton and Barto, 1998).

The competition among multiple agents is, however, neglected in the aforementioned MDP models due to their single-agent setting, resulting in overly optimistic optimal policies. In other words, one agent cannot earn the full amount of the expected reward by following the policy derived in the single-agent setting. In a dynamic environment involving a group of agents, multiple agents interact with both the shared environment and other agents. Multi-agent reinforcement learning (MARL) (Buoniu et al., 2010) thus fits naturally well in this multi-agent system (MAS). Recently, MARL has been attracting significant attention due to its success in tackling high dimensional and complicated tasks such as playing the game of Go (Silver et al., 2016, 2017), Poker (Brown and Sandholm, 2018, 2019), Dota 2 (OpenAI, 2018), and StarCraft II (Vinyals et al., 2019).

MARL tasks can be broadly grouped into three categories, namely, fully cooperative, fully competitive, and a mix of the two, depending on different applications (Zhang et al., 2019): (1) In the fully cooperative setting, agents collaborate with each other to optimize a common goal; (2) In the fully competitive setting, agents have competing goals, and the return of agents sums up to zero; (3) The mixed setting is more like a general-sum game where each agent cooperates with some agents while competes with others. For instance, in the video game *Pong*, an agent is expected to be either fully competitive if its goal is to beat its opponent or fully cooperative if its goal is to keep the ball in the game as long as possible (Tampuu et al., 2017). A progression from fully competitive to fully cooperative behavior of agents was also presented in Tampuu et al. (2017) by simply adjusting the reward.

A key challenge arises in MARL when independent agents have no knowledge of other agents, that is, the theoretical convergence guarantee is no longer applicable since the environment is no longer Markovian and stationary (Matignon et al., 2012; Nguyen et al., 2018). To tackle this issue, one way is to exchange some information among agents. In some contexts, agents actually exchange information with their peers through some coordination. For example, in the game of a team of hunters capturing a team of preys, Tan (1993) proposed multiple ways to enable coordination among agents and concluded that the performance of the hunter agents can be better off through some coordination. However, in other contexts such as the driver repositioning system, agents only have access to their own information. Thus, information exchange among agents involves a central controller which collects the information of all agents and disseminates it to agents. Agents update their value functions and policies based on the provided information from the central controller and their local observations. This is the centralized learning (i.e., based on global information) and decentralized execution (i.e., based on local observation) paradigm, which has become increasingly popular in recent research (Foerster et al., 2016; Lowe et al., 2017; Lin et al., 2018; Li et al., 2019).

While training is stabilized conditioning on the information of other agents such as joint state and joint action in the centralized training paradigm, scalability becomes a critical issue in MARL because the joint state space and joint action space grow exponentially with the number of agents. To make MARL tractable when a large number of agents coexist, Yang et al. (2018) employed the mean field theory to simplify the interaction among agents. The basic idea is, from the perspective of an agent, to treat other agents as a mean agent. Thus, the complexity of interactions among a large number of agents is substantially eased by reducing the dimension in the Q-value function. The large scale MARL with hundreds of or even thousands of agents becomes solvable. To investigate the large-scale order dispatching problem where thousands of agents are present, Li et al. (2019) adopted a mean field approximation and proposed to take the average response from neighboring agents as a proxy of the interaction between the agent and other agents.

Recent studies have successfully applied MARL to multi-driver repositioning and large scale order dispatching problems (Lin et al., 2018; Li et al., 2019; Zhou et al., 2019). Different from treating each driver as an agent in previous studies, Jin et al. (2019) treated each spatial grid as a worker agent and each region composed of several spatial grids as a manager agent and adopted hierarchical reinforcement learning to tackle the joint task of order dispatching and fleet management. All these studies rely on an

underlying assumption that drivers are willing to cooperate under a specifically crafted reward function. For example, embedding the goal of the platform such as improving the gross merchandise volume (GMV) or the order response rate (ORR) into the reward function of a driver encourages cooperation among drivers. Human-drivers are, however, selfish in nature and will only cooperate if the overall return from cooperation is higher than that from competition. This self-interested behavior is utilized to achieve certain degree of cooperation among agents such as adjusting the reward for each agent. However, when the imposed reward function (Lin et al., 2018; Li et al., 2019; Zhou et al., 2019; Jin et al., 2019) is not aligned with the goal of real drivers (e.g., a real driver’s goal can simply be maximizing her monetary return), drivers will not follow the derived optimal policy. Thus, in this work, instead of enforcing a reward function for drivers to cooperate, drivers are regarded as selfish and non-cooperative, and the reward for a driver is simply the monetary return that the driver earns.

Although the approaches in Lin et al. (2018); Li et al. (2019); Zhou et al. (2019); Jin et al. (2019) are efficient under a given reward function, the reached equilibrium is very likely to be a suboptimal from the overall perspective of the system. In this paper, we show that by integrating a reward design mechanism which adjusts the monetary return that a driver earns, a desirable equilibrium can be reached in this intrinsically large-scale non-cooperative system. The desirable equilibrium refers to a Nash equilibrium where each independent and selfish agent’s strategy is the best-response to other agents’ strategies and will produce better overall performance of the system. Mguni et al. (2018) proposed a two-layer architecture with an incentive designer as the upper layer and a potential game as the lower layer and formulated the incentive designers problem as an optimization problem. In contrast, the MARL problem in our context may not be able to be transformed as a potential game, complicating computation of its equilibrium.

In summary, the major contributions of this paper are as follows: (1) Instead of intentionally crafting a reward function, which aligns with the goal of the platform but may not reflect the intrinsic reward of real drivers, this paper takes the monetary return of a driver as the reward function. It aims to improve the performance of the platform by adjusting the monetary return that one driver can earn through a reward design mechanism of the platform (e.g., platform service charge and incentives). (2) With the lower level as the MAS and the upper level as the reward design, this paper formulates a bilevel optimization problem in which a mean field actor-critic algorithm is developed to solve the MAS and a Bayesian optimization algorithm is adopted to efficiently solve the problem.

The remainder of the paper is organized as follows. Section (2) introduces the single-agent actor-critic algorithm, which is a stepping stone for MARL. Section (3) presents the mean field multi-agent reinforcement learning algorithm. Section (4) presents a reward design mechanism and formulates a bilevel optimization problem. Section (5) presents the result and validates the effectiveness of the proposed reward design. Section (6) concludes.

## 2. Single agent reinforcement learning

As a stepping stone, we first introduce the single agent reinforcement learning where only one agent interacts with the environment.

### 2.1. Problem definition

A Markov decision process (MDP) (Puterman, 1994) is typically specified by a tuple  $(S, A, R, P, \gamma)$ , where  $S$  denotes the state space,  $A$  stands for the allowable actions,  $R : S \times A \times S \rightarrow \mathbb{R}$  collects rewards,  $P : S \times A \times S \rightarrow [0, 1]$  denotes a state transition probability from one state to another, and  $\gamma \in [0, 1]$  is a discount factor. A general MDP proceeds simply as follows. Starting from the initial state, the agent specifies an action  $a \in A$  whenever the agent is in a state  $s \in S$ . The agent then transits into a new state  $s' \in S$  with probability  $P(s'|s, a)$  and observes an immediate reward  $r(s, a, s')$  by obeying the dynamics of the environment. Then the process repeats until a terminal state is reached. A policy  $\pi : S \times A \rightarrow [0, 1]$  simply maps from state  $s \in S$  to the probability of taking action  $a \in A$  in state  $s$ , i.e.,  $\pi(a|s)$ . The goal of solving an MDP is to derive an optimal policy  $\pi^*$  so that the agent can maximize her long term expected reward by following the policy. In reinforcement learning problems, the transition probability matrix  $P$  is commonly unknown, and the agent learns about  $P$  from its interaction with the environment.

Denote  $V^\pi(s)$  as the state value, which is the expected cumulative reward that an agent can earn by starting from state  $s$  and following a policy  $\pi$ .  $V^\pi$  can be recursively given as (Sutton and Barto, 1998)

$V^\pi(s) = \mathbb{E}_{a \sim \pi(\cdot|s), s' \sim P(\cdot|s,a)} [r(s, a, s') + \gamma V^\pi(s')]$ . Denote  $Q^\pi(s, a)$  as the state-action value, which is the expected cumulative reward that an agent can earn by starting from state  $s$ , taking action  $a$ , and following a policy  $\pi$ .  $Q^\pi$  is related with  $V^\pi$  through  $Q^\pi(s, a) = \mathbb{E}_{s' \sim P(\cdot|s,a)} [r(s, a, s') + \gamma V^\pi(s')]$ .

The optimal value  $V$  can then be written as  $V(s) = \max_a V^\pi(s), \forall s \in S$ . The Bellman optimality equation is given as (Sutton and Barto, 1998):

$$V(s) = \max_a \mathbb{E}_{s' \sim P(\cdot|s,a)} [r(s, a, s') + \gamma V(s')],$$

where the optimal state-action value is  $Q(s, a) = \mathbb{E}_{s' \sim P(\cdot|s,a)} [r(s, a, s') + \gamma V(s')]$ .

Our task is then to derive an optimal policy  $\pi^*$  (i.e., to solve the MDP) with which the agent can optimize its expected cumulative reward.

To demonstrate how to apply MDPs problems to the context of e-hailing driver reposition, we will use examples on a 2-by-2 grid world throughout the paper every time when models are introduced.

**Example 2.1.** (Single-Agent  $2 \times 2$ ). The single-agent driver reposition is presented in Figure (1). We adopt a grid world setup where the index of each grid (denoted as  $l$ ) is shown at the upper left corner. The taxi icon denotes the driver, and the person icon is the passenger request with the corresponding fare shown above. The time beneath the driver and the passenger request records the current time of the driver and the appearance time of the passenger request, respectively. The dashed line with arrow shows the origin and destination of the passenger request.

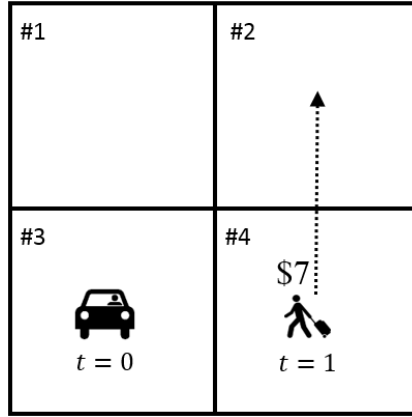


Figure 1: An illustrative example (Single agent)

*S.* The state of the driver consists of two components, namely, the grid index  $l$  and current time  $t$ , i.e.,  $s = (l, t)$ . For instance, the current state of the driver is  $s = (\#3, 0)$  in this example.

*A.* The allowable action of the driver is either moving into one of the neighboring grids or staying within the current grid. To be concise, we use the index of grid where the driver chooses to enter as the action. Suppose the driver decides to go rightward in the example, then we can denote  $a = \#4$ . We further assume it takes the driver one time step to enter grid  $\#4$ . In other words, the current time of the driver is  $t = 1$  when the driver arrives in grid  $\#4$ .

*P.* Considering the driver arrives in grid  $\#4$  at time  $t = 1$ , and at the same time a passenger request appears in grid  $\#4$  with 80% probability. If this driver is matched to the passenger and picks up the passenger, the driver will transit to the passenger's destination, which is grid  $\#2$ . Denote the transition time from grid  $\#4$  to grid  $\#2$  as  $\Delta t_{\#4 \rightarrow \#2}$ . We can define the new state  $s' = (\#2, 1 + \Delta t_{\#4 \rightarrow \#2})$ . Then the transition probability from the state  $s$  at time 1 to the state  $s'$  at time  $1 + \Delta t_{\#4 \rightarrow \#2}$  is 80%, mathematically,  $P(s'|s, a) = 80\%$ . If there is no passenger request in grid  $\#4$  at time  $t = 1$ , then the driver ends up in state  $s' = (\#4, 1)$ . The transition probability becomes  $P(s'|s, a) = 20\%$ .

*R.* If we take the fare of the fulfilled passenger request as the reward,  $r(s, a, s') = \$7$  in the example. Based on the received reward at this step and the future cumulative reward, the driver chooses an action in the new state  $s'$ , and the state transition process repeats until a terminal state (i.e.,  $t = T$  where  $T$  is a predefined ending time, say, the end of the driver's work time) is reached.  $\square$

## 2.2. Actor-Critic method

To solve optimal policies, there are two types of methods, namely, value based or critic-only method and policy based or actor-only method. Value based and policy based methods are commonly used termi-

nologies, but from now on we will use critic-only and actor-only methods for the purpose of introducing the actor-critic method.

Critic-only methods aim to output the optimal policy  $\pi$  through optimizing the state-action  $Q(s, a)$  or the state value  $V(s)$ . Actor-only methods directly output an optimal policy  $\pi$  without resorting to stored value functions  $Q(s, a)$  or  $V(s)$  as an intermediary. Both methods have pros and cons. Critic-only methods enjoy a low variance in the estimate of the state-action value but may lack guarantees on the optimality or near-optimality of the resulting policy if an optimal policy cannot be easily solved from value functions. Actor-only methods work well on continuous and large action spaces but may suffer from high fluctuation in policies (Konda and Tsitsiklis, 2003; Grondman et al., 2012). To overcome the shortcomings of these methods, actor-critic methods are developed to combine strengths of both methods (Konda and Tsitsiklis, 2003).

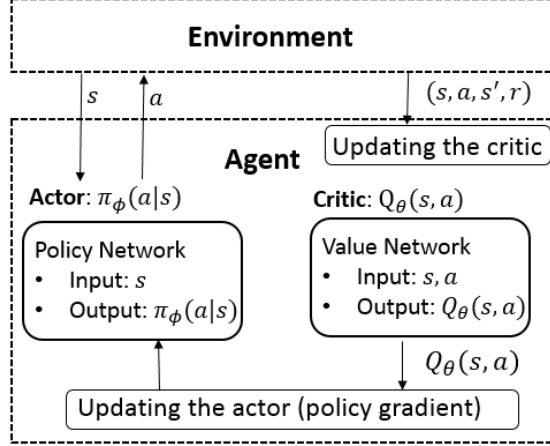


Figure 2: Actor-critic algorithm

Figure (2) presents the architecture of the actor-critic algorithm. One agent, who has an actor and a critic, interacts with the environment. The agent observes its state  $s$  from the environment and inputs  $s$  to the actor that outputs the policy, i.e., a probability distribution over all possible actions. The agent samples an action  $a$  from the probability distribution and takes action  $a$  in the environment. Then the agent observes a state transition  $s \rightarrow s'$  and receives a reward  $r$  from the environment. Based on the one-step transition  $s \rightarrow s'$  as well as action  $a$  and reward  $r$ , the agent updates its critic. With the updated Q-value  $Q_\theta(s, a)$ , the agent updates its actor using policy gradient. Now we detail both the critic and the actor, respectively.

**Critic.** The critic takes as input state  $s$  and action  $a$  and outputs Q-value  $Q(s, a)$ . Q-learning is the most commonly used algorithm to update the Q value based on the state transition  $s \rightarrow s'$  with reward  $r(s, a, s')$  and updates the Q-value by

$$Q(s, a) \leftarrow Q(s, a) + \eta[r(s, a, s') + \gamma \max_{a'} Q(s', a') - Q(s, a)] \quad (1)$$

where  $\eta$  is the learning rate and  $0 < \eta \leq 1$ . If  $\eta$  reduces over time properly, the Q-learning update converges (Sutton and Barto, 1998). Equation (1), however, is only applicable to a finite and discrete state and action space. In other words, one needs to maintain a Q table with all possible combinations of  $s$  and  $a$ , which is not tractable for a continuous and large state and action space. Therefore we need functional approximation to the original Q-value. Deep neural network, i.e., deep Q network (DQN), is one of the most popular value approximator (Mnih et al., 2015). Denote a deep neural network parameterized by  $\theta$  as  $Q_\theta(s, a)$ , to approximate  $Q(s, a)$ . DQN updates its parameter  $\theta$  by minimizing the loss

$$\mathcal{L}(\theta) = \mathbb{E}_{s, a, s'} [\underbrace{(r(s, a, s') + \gamma \max_{a'} Q_\theta(s', a') - Q_\theta(s, a))}_{\text{target}}]^2. \quad (2)$$

This problem can be solved by the gradient descent method, whose gradient is straightforward to compute as follows:  $\nabla_\theta \mathcal{L}(\theta) = \mathbb{E}_{s, a, s'} [-\nabla_\theta Q_\theta(s, a) \times (r(s, a, s') + \gamma \max_{a'} Q_\theta(s', a') - Q_\theta(s, a))]$ , where the gradient is not taken with respect to the target.

**Actor.** The actor takes as input state  $s$  and outputs a probability distribution on all allowable actions in this state. Similarly to how we use a value network to approximate Q-value, we can also use a deep neural network, i.e., policy network, to approximate the policy  $\pi$ . Denote the policy network parameterized by  $\phi$  as  $\pi_\phi(a|s)$ . The goal of the actor is to maximize its expected cumulative reward, denoted as  $\rho(\pi_\phi) = \sum_{t=0}^T \gamma^t r^t$ , where  $r^t$  is the reward the actor receives at time  $t$ . To solve the optimal policy of the actor requires us to know its gradient. The gradient of the policy is complicated to solve and is given as (Sutton et al., 1999)

$$\nabla_\phi \rho(\pi_\phi) = \mathbb{E}_{s,a} [\underbrace{(Q^{\pi_\phi}(s,a) - b^{\pi_\phi}(s))}_{\text{advantage}} \nabla_\phi \log(\pi_\phi(a|s))], \quad (3)$$

where  $Q^{\pi_\phi}$  denotes the Q-value function following the policy  $\pi_\phi$ ,  $b^{\pi_\phi}$  is some baseline (e.g.,  $b^{\pi_\phi} = V^{\pi_\phi}$ , i.e., the value function following the policy  $V^{\pi_\phi}$ ), and  $Q^{\pi_\phi}(s,a) - b^{\pi_\phi}(s)$  is called the advantage of a taken action  $a$ , a measure of the goodness of an action. If it is greater than zero, it means this taken action is generally good, otherwise it may be bad. Naturally, the underlying rationale in computing the policy gradient defined in Equation (3) is to update the policy distribution to concentrate on potentially good action(s). When the chosen action  $a$  leads to a positive advantage, i.e.,  $Q^{\pi_\phi}(s,a) - b^{\pi_\phi}(s) > 0$ , the policy is updated towards the direction of favoring action  $a$ . When the advantage is negative for action  $a$ , the policy is updated in the direction of against action  $a$ .

To summarize, in addition to the policy network  $\pi_\phi$ , the actor-critic algorithm also maintains a value network  $Q_\theta$  so that the calculation of the gradient of the policy in Equation (3) directly uses the Q-function approximator  $Q_\theta$ , to ensure stability of policy update. The actor-critic algorithm simultaneously updates critic (by minimizing the loss given in Equation (2)) and the actor (by the gradient given in Equation (3)) as more samples are fed in.

### 3. Multi-agent reinforcement learning

To tackle a real-world problem with multiple agents, the aforementioned single agent reinforcement learning falls short of capturing the coupling effects or the competition among multiple agents. In this section, we introduce a mean field multi-agent reinforcement learning approach to model the multi-driver repositioning task.

#### 3.1. Problem definition

The multi-agent problem is modeled as a partially observable Markov decision process (POMDP) (Littman, 1994), defined by a tuple  $(S, O_1, O_2, \dots, O_N, A_1, A_2, \dots, A_N, P, R_1, R_2, \dots, R_N, N, \gamma)$ , where  $N$  is the number of agents and  $S$  is the environment state space. Environment state  $\mathbf{s} \in S$  is not fully observable. Instead, agent  $i$  draws a private observation  $o_i \in O_i$  which is correlated with  $\mathbf{s}$ .  $O_i$  is the observation space of agent  $i$ , yielding a joint observation space  $O = O_1 \times O_2 \times \dots \times O_N$ ,  $A_i$  is the action space of agent  $i \in \{1, 2, \dots, N\}$ , yielding a joint action space  $A = A_1 \times A_2 \times \dots \times A_N$ ,  $P : S \times A \times S \rightarrow [0, 1]$  is the state transition probability,  $R_i : S \times A \times S \rightarrow \mathbb{R}$  is the reward function for agent  $i$ , and  $\gamma$  is the discount factor.

Agent  $i \in \{1, 2, \dots, N\}$  uses a policy  $\pi_i : O_i \times A_i \rightarrow [0, 1]$  to choose actions after drawing observation  $o_i$ . After all agents taking actions, the joint action  $\mathbf{a}$  triggers a state transition  $\mathbf{s} \rightarrow \mathbf{s}'$  based on the state transition probability  $P(\mathbf{s}'|\mathbf{s}, \mathbf{a})$ . Agent  $i$  draws a private observation  $o'_i$  corresponding to  $\mathbf{s}'$  and receives a reward  $r_i(\mathbf{s}, \mathbf{a}, \mathbf{s}')$ . Agent  $i$  aims to maximize its discounted expected cumulative reward by deriving an optimal policy  $\pi_i^*$  which is the best response to other agents' policies. This process repeats until agents reach their own terminal state.

Due to the existence of other agents, the Q-value function for agent  $i$ , i.e.,  $Q_i$ , is now dependent on the environment state  $\mathbf{s} \in S$  and the joint action  $\mathbf{a} \in A$  of all agents, i.e.,

$$Q_i = Q_i(\mathbf{s}, \mathbf{a}). \quad (4)$$

Similarly, the value function of agent  $i$ , i.e.,  $V_i = V_i(\mathbf{s})$ , is dependent on the environment state  $\mathbf{s}$ .

Subsequently, we will demonstrate how to formulate the multi-driver repositioning problem in MARL, building on the single-agent example developed in the previous section.

**Example 3.1.** (Multi-Agent  $2 \times 2$ ). The multi-agent driver reposition is presented in Figure (3). Same as before, a grid world setup is adopted. Now we have two drivers with their indices shown above the taxi icon and two passenger requests with fare presented above the passenger icon. The time beneath drivers and passenger requests records the current time of the driver and the appearance time of the passenger request, respectively. The dashed line with arrow shows the origin and destination of the passenger request.

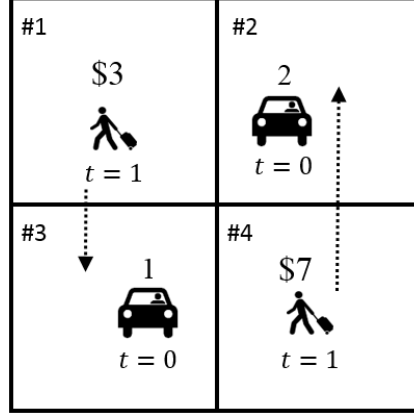


Figure 3: An illustrative example (Multi agent)

*N.* There are  $N = 2$  drivers moving around in the environment. We denote drivers by  $\{1, 2\}$ .

*S.* The environmental state consists state information of both drivers. For driver  $i$ , her state  $s_i$  is composed of her current location  $l_i$  (i.e., the grid index based on a grid world setup) and current time  $t$ , i.e.,  $s_i = (l_i, t)$ . The joint state of both drivers, i.e., the environment state  $\mathbf{s} \in S$ , at time  $t$  is denoted as  $\mathbf{s} = (s_1, s_2)$ . In this example, at current time  $t = 0$ ,  $\mathbf{s} = ((\#3, 0), (\#2, 0))$ .

*A.* For driver  $i$ , her action  $a_i \in A_i$  can be any of the five possible actions, i.e., moving into any of her four neighboring grids or staying in the current grid. The same as before, we use the index of grid where the driver chooses to enter as the action. The joint action of both drivers is  $\mathbf{a} = (a_1, a_2)$ . Assuming driver 1 decides to go rightward (i.e., to enter grid #4) and driver 2 chooses to go leftward (i.e., to enter grid #1), the joint action is  $\mathbf{a} = (\#4, \#1)$ . We further assume it then takes driver 1 one time step to enter grid #4 and driver 2 one time step to enter grid #1. In other words, after driver 1 arrives in grid #4 and driver 2 arrives in grid #1, the clock ticks one step forward and the current time is now  $t = 1$ .

*P.* The joint action  $\mathbf{a}$  triggers a state transition  $\mathbf{s} \rightarrow \mathbf{s}'$  with some probability according to the state transition function, i.e.,  $P(\mathbf{s}'|\mathbf{s}, \mathbf{a})$ . Driver 1 gets matched to the passenger request in grid #4 at  $t = 1$ , loads up the passenger, and drives to the destination of the passenger. Driver 1 then arrives in a new state  $s'_1 = (\#2, 1 + \Delta t_{\#4 \rightarrow \#2})$  where  $\Delta t_{\#4 \rightarrow \#2}$  is the transition time from grid #4 to grid #2. Driver 2 gets matched to the passenger request in grid #1 at  $t = 1$ , loads up the passenger, and drives to the destination of the passenger. Driver 2 then arrives in a new state  $s_2 = (\#3, 1 + \Delta t_{\#1 \rightarrow \#3})$  where  $\Delta t_{\#1 \rightarrow \#3}$  is the transition time from grid #1 to grid #3.  $\mathbf{s}' = ((\#2, 1 + \Delta t_{\#4 \rightarrow \#2}), (\#3, 1 + \Delta t_{\#1 \rightarrow \#3}))$ . In this simple example,  $P(\mathbf{s}'|\mathbf{s}, \mathbf{a}) = 1$  due to the deterministic appearance of passenger requests.

*R.* Along with the state transition, each driver receives a reward, i.e.,  $r_i$ . The reward function  $r_i$  for each agent  $i \in \{1, 2\}$  is simply the fare of the fulfilled passenger request, i.e.,  $r_1 = \$7$  and  $r_2 = \$3$ .  $\square$

This example will be revisited later in this section to illustrate the algorithm.

### 3.2. Techniques to simplify the Q-value function

The dependency of the Q-value of an agent  $i$  on other agents' states and actions, as shown in Equation (4), however, introduces prohibitively high difficulties in learning the optimal Q-value. The main reasons are two-fold. First, although each agent draws its private observation  $o_i$  from the environment state  $\mathbf{s}$ ,  $\mathbf{s}$  cannot be observed by any agent, i.e.,  $\mathbf{s}$  is unknown. Second, one agent does not observe the actual actions taken by all agents, i.e.,  $\mathbf{a}$  is unknown.

To make the Q-value of an agent in the multi-agent system tractable, the dependency of the Q-value on the environment state  $\mathbf{s}$  and joint action  $\mathbf{a}$  needs to be simplified. A very natural approach, inspired by the single-agent setting, is independent learning where each agent  $i$  only has information about its

own observation  $o_i$  and action  $a_i$  but has no information about other agents. Thus, the Q-value function of agent  $i$  is reduced to

$$Q_i = Q_i(o_i, a_i). \quad (5)$$

In other words, private observations and joint action of other agents are not used by agent  $i$ . After all agents choosing actions, the joint action  $\mathbf{a}$  triggers a state transition. Agent  $i$  then draws a new private observation  $o'_i$  and receives a reward  $r_i$ .

The independent learning algorithm, although is intuitive and simple, can be unstable and hard to reach convergence since the environment is no longer Markovian and stationary due to the appearance of other agents (Matignon et al., 2012).

### 3.2.1. Centralized training and decentralized execution

To make the training more stable and ensure convergence, we employ the centralized training and decentralized execution paradigm (Foerster et al., 2016; Lowe et al., 2017; Lin et al., 2018; Li et al., 2019). In this paradigm, to train the policy of agents, we assume these agents know the global information such as the joint observation and/or joint action. In other words, in addition to observation  $o_i$  and action  $a_i$ , agent  $i$  also has access to the observations and/or actions of other agents during training. While in the execution phase, decentralized testing or execution is implemented, meaning they would not have access to the global information anymore. To realize this paradigm, the aforementioned actor-critic algorithm naturally fits in, because we can apply global information to the critic, i.e., joint observation and joint action in  $Q_i$ , in the training phase, while feeding local information to the actor, i.e.,  $o_i$  in  $\pi_i$ , in the execution phase. Decentralized execution becomes possible because only actors are used in execution.

Then the Q-value function of agent  $i$  becomes

$$Q_i = Q_i(o_i, o_{-i}, a_i, a_{-i}), \quad (6)$$

where  $o_{-i} = (o_1, \dots, o_{i-1}, o_{i+1}, \dots, o_N)$  and  $a_{-i} = (a_1, \dots, a_{i-1}, a_{i+1}, \dots, a_N)$  denote the joint observation and joint action of all agents except agent  $i$ , respectively.

In the context of e-hailing driver repositioning, considering the definition of the action, which is the index of the grid where the driver chooses to enter, the Q-value function of driver  $i$ , i.e.,  $Q_i$ , does not depend on the joint observation of other drivers, i.e.,  $o_{-i}$ . Explanations are as follows. When driver  $i$  chooses action  $a_i = l$  based on its observation  $o_i$ , driver  $i$  then enters grid  $l$ . At the same time, other drivers also enter some grid based on their joint action  $a_{-i}$  regardless of their joint observation  $o_{-i}$ . The Q-value function of driver  $i$  only depends on the current distribution of drivers, which has been determined by their joint action  $a_{-i}$ . Therefore it is the joint action  $a_{-i}$  which affects  $Q_i$ . The Q-value function is thus further reduced to

$$Q_i = Q_i(o_i, a_i, a_{-i}). \quad (7)$$

### 3.2.2. Mean field approximation

The centralized training and decentralized execution paradigm, however, can easily become intractable due to the exponential increase in the joint action space with the increasing number of agents. For example, the size of the joint action space easily blows up for  $N$  agents with  $|A|$  possible actions (i.e.,  $|A|^N$  possibilities). To simplify the interaction among agents, we adopt the mean field approximation. The basic idea of the mean field approximation is to simplify the complicated interaction between one agent and all other agents by a pairwise interaction between the agent and a virtual mean agent which is formed by the neighboring agents of the agent. Thus, the complexity of interactions among a large number of agents is substantially eased by reducing the dimension in the input of the Q-value function. Therefore the large scale MARL with hundreds of or even thousands of agents becomes solvable.

To be more precise, we provide brief explanations that lead to the applicability of the mean field approximation in MARL as described in Yang et al. (2018). First, from the perspective of agent  $i$ , the multi-agent effect or competition effect mainly comes from its neighboring agents, i.e.,  $Q_i(o_i, a_i, a_{-i}) \approx \frac{1}{N_i} \sum_{k \in N(i)} Q_i(o_i, a_i, a_k)$ , where  $N(i)$  denotes the neighboring agents of agent  $i$ . However, it is still cumbersome to compute  $Q_k, k \in N(i)$  for the neighboring agents of agent  $i$  if this number is large. Define a mean action  $\bar{a}_i$ , which is a proxy of the actions taken by the neighboring agents. Accordingly,  $Q_i(o_i, a_i, a_{-i})$  can be further simplified to  $Q_i(o_i, a_i, \bar{a}_i)$  when Taylor expansion is applied, which is

$$Q_i \approx \frac{1}{N_i} \sum_{k \in N(i)} Q_i(o_i, a_i, a_k) \approx Q_i(o_i, a_i, \bar{a}_i). \quad (8)$$



Interested readers can refer to Yang et al. (2018) for a detailed explanation and proof.

**Example 3.2.** (Multi-Agent  $2 \times 2$ ). The mean action  $\bar{a}_i$  of the neighboring drivers of driver  $i$  is defined as the demand to supply ratio in the grid where driver  $i$  is entering. Assuming both drivers choose action #4, i.e.,  $a_1 = a_2 = \#4$  in the multi-agent  $2 \times 2$  example shown in Figure (3), there are 2 drivers and 1 passenger request in grid #4 after both drivers enter grid #4. The mean action for both drivers is thus  $\bar{a}_1 = \bar{a}_2 = \frac{1}{2} = 0.5$ . This definition of mean action captures the level of competition in a grid. A larger mean action  $\bar{a}_i$  denotes a higher demand to supply ratio and lower level of competition, and vice versa.  $\square$

### 3.3. Mean field actor-critic algorithm

As previously mentioned, each agent  $i \in \{1, 2, \dots, N\}$  maintains a policy network  $\pi_i$  (i.e., the actor) and a Q-value network  $Q_i$  (i.e., the critic). For a real-world multi-agent task, there are typically hundreds of or even thousands of agents, indicating that maintaining two deep neural networks (i.e., one for the actor and one for the critic) per agent is not computationally tractable. Considering that for a class of multi-agent tasks where anonymous agents share the same state space, action space, and reward function, agents are thus homogeneous. The multi-agent task can then be largely simplified by sharing both the actor and the critic among drivers, i.e.,  $Q_1 = Q_2 = \dots = Q_N = Q$  and  $\pi_1 = \pi_2 = \dots = \pi_N = \pi$ .

After adopting the mean field approximation, the loss function for the critic, which was presented in Equation (2) for the single-agent setting, now becomes

$$\mathcal{L}(\theta) = \mathbb{E}_{o_i, a_i, o'_i} (r(o_i, a_i, o'_i) + \gamma \max_{a'_i} \mathbb{E}_{\bar{a}'_i} [Q_\theta(o'_i, a'_i, \bar{a}'_i)] - Q_\theta(o_i, a_i, \bar{a}_i))^2. \quad (9)$$

The only difference is the incorporation of the mean action  $\bar{a}$  into the Q-value function approximation. Similarly, the gradient of the policy, which was presented in Equation (3) for single-agent setting, is now

$$\nabla_\phi \rho(\pi_\phi) = \mathbb{E}_{o_i, a_i} [(\mathbb{E}_{\bar{a}} [Q_\theta(o_i, a_i, \bar{a}_i)] - V(o_i)) \nabla_\phi \log(\pi_\phi(a_i | o_i))]. \quad (10)$$

---

#### Algorithm 1 Mean field actor-critic algorithm

---

- 1: Initialize a deep neural network  $Q_\theta(o, a, \bar{a})$ , parameterized by  $\theta$ , for the critic and a deep neural network  $\pi_\phi(a|o)$ , parameterized by  $\phi$ , for the actor
  - 2: Initialize  $\epsilon = \epsilon_0$ , which is the parameter associated with random exploration
  - 3: Initialize the learning rate  $\eta = \eta_0$
  - 4: **repeat**
  - 5:   Randomly initialize a starting grid for all agents, and each agent  $i \in \{1, 2, \dots, N\}$  draws a private observation  $o_i$
  - 6:   Set  $t = 0$
  - 7:   **repeat**
  - 8:     Sample a value  $x$  from a uniform distribution which is defined on  $[0, 1]$
  - 9:     **if**  $x < \epsilon$  **then**
  - 10:       Select an action  $a_i$  from the allowable action space randomly for all available agents
  - 11:     **else**
  - 12:       Select an action  $a_i$  greedily according to the policy  $\pi$  for all available agents
  - 13:     **end if**
  - 14:     Each available agent takes its action  $a_i$ , observes a reward  $r_i$  and draws a new observation  $o'_i$
  - 15:      $t \leftarrow t + 1$
  - 16:   **until**  $t = T$
  - 17:   Update the critic  $Q$  by minimizing the loss defined Equation (9)
  - 18:   Update the actor  $\pi$  using the gradient defined in Equation (10)
  - 19:   Decrease the exploration parameter  $\epsilon$
  - 20:   Decrease the learning rate  $\eta$
  - 21: **until** the algorithm converges
  - 22: Return the optimal policy  $\pi$
- 

**Example 3.3.** (Multi-Agent  $2 \times 2$ ). Now we apply the mean field actor-critic algorithm to the multi-driver example shown in Figure (3). Figure (4) presents the architecture of the mean field actor-critic

algorithm particularly for the context of multi-driver repositioning. Homogeneous agents, who share a common actor and a common critic, interact with the environment. The shared actor is a multilayer perceptron with 32 neurons in its hidden layer and takes as input observation  $o_i$  and outputs a five dimensional vector denoting the probability distribution of taking five actions. Similarly, the shared critic takes as input  $(o_i, a_i, \bar{a}_i)$  and outputs the Q-value. During training, agent  $i \in \{1, 2, \dots, N\}$  draws its private observation  $o_i$  from the environment and inputs  $o_i$  to the actor which outputs a probability distribution over actions. Agent  $i$  samples an action  $a_i$  from the probability distribution and takes the sampled action in the environment. Joint action of all agents  $\mathbf{a}$  triggers a state transition  $\mathbf{s} \rightarrow \mathbf{s}'$  in the environment. Agent  $i$  then observes the mean action  $\bar{a}_i$ , draws a new observation  $o'_i$ , and receives a reward  $r_i$  from the environment. The agent then uses  $(o_i, a_i, o'_i, r_i, \bar{a}_i)$  to update the shared critic by minimizing the loss presented in Equation (9). Based on the advantage calculated from the critic, agent  $i$  updates the shared actor using the gradient presented in Equation (10).

The aforementioned training process is centralized because the mean action used in the critic is actually some global information. During execution, agents only need to use the updated actor, which only takes as input the local information, i.e., the private observation. In other words, the shared critic is not used in execution.

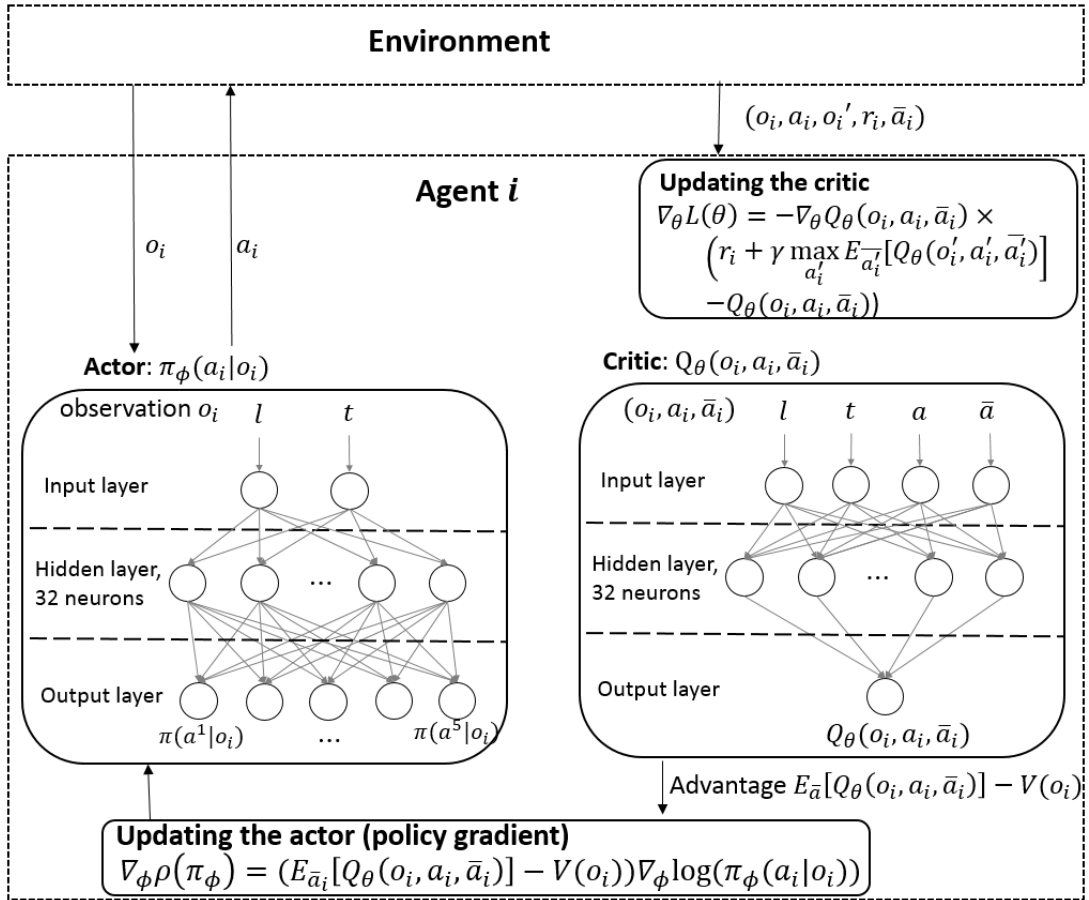


Figure 4: Mean field actor-critic algorithm for multi-driver repositioning

The derived Q values corresponding to four scenarios of interest are presented in Figure (5). In Figure (5a), when both drivers choose action #4, the observed mean action for both of them is the ratio of demand to supply, i.e.,  $\bar{a}_1 = \bar{a}_2 = \frac{1 \text{ passenger request}}{2 \text{ drivers}} = 0.5$ . The resulting expected value for both drivers is \$3.5, i.e.,  $Q(o_1, a_1, \bar{a}_1) = Q(o_2, a_2, \bar{a}_2) = 3.5$ , because both of them have an equal probability  $\frac{1 \text{ driver}}{2 \text{ drivers}} = 50\%$  to take the passenger request with \$7. Similarly, the observed mean actions and resulting Q values can be explained in other scenarios. The Q-value bimatrix is presented in Table (1) where driver 1 is the column player and driver 2 is the row player. When driver 1 chooses action #1 and driver 2

chooses action #1, Q-values for them are 1.5 and 1.5, respectively, according to Figure (5d). Similarly, Q-values for both drivers can be read from Figure (5) for other scenarios. Based on the bimatrix, driver 1 always chooses action #4 because action #4 is strictly better than action #1 regardless of the observed mean action, and driver 2 always chooses action #4 for the same reason. Thus, the optimal policy for both drivers is to enter grid #4 with an expected payoff \$3.5.

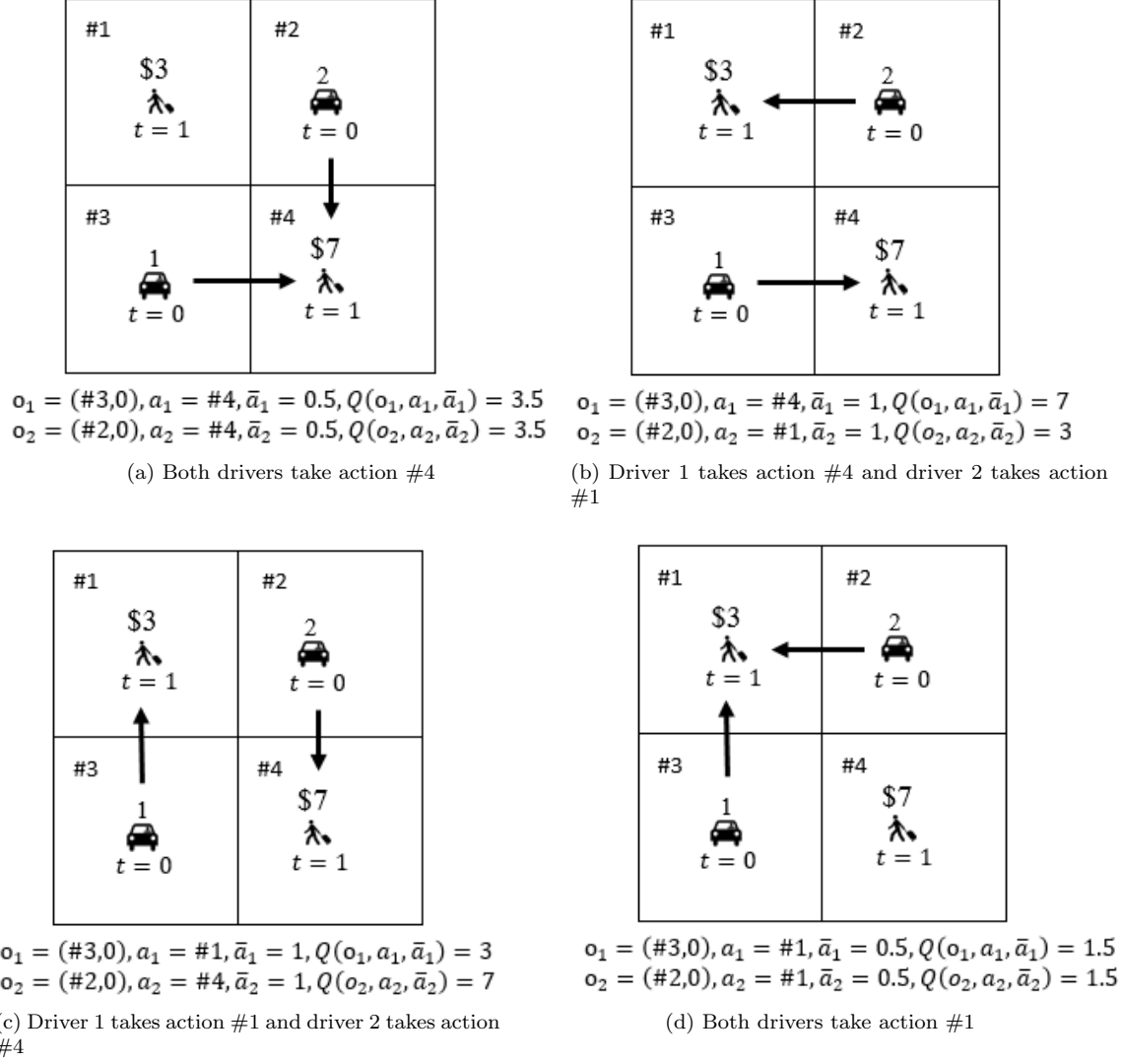


Figure 5: Derived Q values for four scenarios of interest

Table 1: Q-value bimatrix for drivers

		Driver 1	
		#1	#4
Driver 2	#1	1.5, 1.5 (Figure 5d)	7, 3 (Figure 5b)
	#4	3, 7 (Figure 5c)	3.5, 3.5 (Figure 5a)

#### 4. Reward design for multi-agent reinforcement learning

Due to selfishness of each agent, performing MARL under a given reward function in an MAS is very likely to yield an undesirable equilibrium from the perspective of the system. In other words, this equilibrium may not be an optimum with respect to some system objectives. To guide a multi-agent

system towards a desirable equilibrium, system planners could resort to reward design mechanisms by modifying the reward function of agents. In this paper, we introduce a new parameter  $\alpha \in \mathcal{A}$  into agents' reward, where  $\mathcal{A}$  is the feasible domain of  $\alpha$ . Parameter  $\alpha$  can be either a scalar or a vector. The goal of system planners is to maximize some system performance measure dependent of  $\alpha$ , denoted as  $f(\alpha)$ . The system planner first chooses a value of  $\alpha$  and inputs  $\alpha$  to the MAS. With the given  $\alpha$  which determines the reward, the developed mean field actor-critic algorithm is employed to derive an optimal policy  $\pi$ , which is dependent on  $\alpha$ , for all agents in the system. Some performance measure  $f$ , which is calculated by executing the derived optimal policy  $\pi$  for all agents, is then fed into the reward design. The performance measure  $f$  is dependent on  $\alpha$  through the dependency of  $\pi$  on  $\alpha$ . In other words,  $f = f(\alpha)$ .

In summary, the reward design problem is to select a parameter  $\alpha$  to maximize the performance measure  $f(\alpha)$  on the upper level, while the distributed agents aim to maximize their individual cumulative rewards on the lower level once  $\alpha$  is given as part of their reward. This process can be formulated as a bi-level optimization problem, mathematically,

$$\begin{aligned} & \max_{\alpha \in \mathcal{A}} f(\alpha) \\ & \text{where} \end{aligned} \tag{11}$$

$$\max_{\pi} \sum_{k=t}^T \gamma^{k-t} r_i^k(\alpha), \forall t \in \{0, 1, \dots, T\}, \forall i \in \{1, 2, \dots, N\}$$

The interaction between upper and lower levels through exchange of variables is shown in Figure (6).

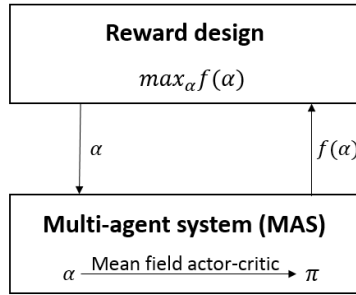


Figure 6: Architecture of the reward design

The optimization problem presented in Equation (11), however, is not straightforward to solve due to the unknown complex structure of  $f$  over the parameter  $\alpha$ . The traditional gradient based method such as gradient descent is thus no longer applicable.

In this paper, we adopt Bayesian optimization (hereafter we call it BO). The procedure of BO is as follows. First, BO places a statistical model on the objective function  $f$ , such as a Gaussian process. Second, BO devises an acquisition function to decide where to evaluate next, i.e., to choose an  $\alpha$  based on the statistical model. Third, BO updates the statistical model based on the newly evaluated  $\alpha$ , and the process repeats. The pseudo-code of BO is listed in Algorithm (2). Interested readers are referred to (Frazier, 2018) for more details on BO.

---

#### Algorithm 2 Bayesian Optimization

---

- 1: Initialize a Gaussian process prior on  $f$
  - 2: Evaluate  $f$  at  $n_0$  different  $\alpha$ s according to certain rules
  - 3: Set computational budget  $\mathcal{N}$  and  $n = n_0$
  - 4: **while**  $n \leq \mathcal{N}$  **do**
  - 5:   Update posterior probability distribution on  $f$  based on all evaluated  $\alpha$ s
  - 6:   Calculate an acquisition function
  - 7:   Locate the  $\alpha_n$  which maximizes the acquisition function
  - 8:   Evaluate  $f$  at  $\alpha_n$
  - 9:    $n \leftarrow n + 1$
  - 10: **end while**
  - 11: Return  $\alpha_n$  which maximizes  $f$
-

To be more concrete, now we use the multi-agent  $2 \times 2$  example presented in Figure (3) to illustrate the potential of the reward design.

**Example 4.1.** (Multi-Agent  $2 \times 2$ ). We take the order response rate (ORR), i.e. the ratio of the number of fulfilled passenger requests to the total number of passenger requests, as the performance measure of the system. The direct application of mean field actor-critic algorithm yields a 50% ORR, which is obviously not the desired equilibrium from the perspective of the system. Noticing that the platform typically charges a certain proportion of the fare paid by the passenger as the so-called platform service charge, which is reportedly to be dependent on various factors such as distance, duration, and city. We aim to improve the performance of the system by devising a proper reward design.

In Figure (3), trip fares are shown right above each passenger request, the reached equilibrium for both drivers without any charge are to enter grid #4 and get an expected reward as \$3.5, leading to an oversupply (i.e., a low demand to supply ratio) in grid #4 and an undersupply (i.e., a high demand to supply ratio) in grid #1, which is not beneficial for the system. A reward design which deducts \$1.1 from the passenger request paid to the driver in grid #4 will effectively attract one driver to leave grid #4 for grid #1 to get more monetary return, resulting in a 100% order response rate.

## 5. Case Study

We test the bilevel optimization model on a 2-by-2 grid world example, where an analytical solution of the reward design can be derived. Then we compare both values to justify the correctness of our BO algorithm.

The dataset consists of seven deterministic passenger requests in a 2-by-2 grid world setup, as shown in Figure (7). At  $t = 0$ , there are five idle drivers in grid #2 and five in grid #3. At time  $t = 1$ , five passenger requests with fare \$10 deterministically appear in grid #4 and two passenger requests with fare \$4.9 appear in grid #1.

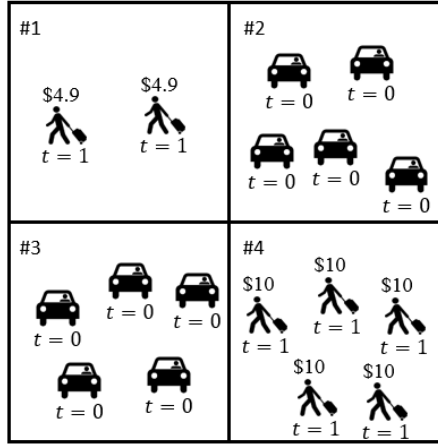


Figure 7: Layout

Without any reward design, the optimal policy for all drivers is to enter grid #4, because the expected return for entering grid #4 is at least \$5 (i.e.,  $\frac{\$10 \times 5}{10}$ ) while that for entering grid #1 is at most \$4.9. The resulting ORR is  $5/7 = 71.43\%$ , which is not desirable from the perspective of the platform because it is expected to achieve a 100% ORR in this setting. Actually, the platform can achieve a better ORR by adjusting the reward that drivers earn through the use of a platform service charge (aka the commission fee). The platform service charge used in this study is denoted as a fare percentage. For instance, a 10% service charge means the platform takes 10% of the fare paid by the passenger to the driver as its revenue. In other words, the driver gets less money under a higher service charge while the payment from the passenger remains the same. To achieve a better ORR, the platform needs to place a high service charge in grids which are oversupplied. Drivers oversupply grid  $l$  because on average they can earn more by entering grid  $l$ , compared with entering other grids. A high service charge placed in grid  $l$  can effectively reduce monetary returns for drivers entering  $l$  and make grid  $l$  less attractive to drivers. Thus, some drivers choose other grids and take other passenger requests, resulting in an increase in ORR.

Before introducing a functional form of the platform service charge, we formally provide two notations, namely demand to supply ratio (DS) and service charge (SC). We then construct an effective form of SC as a function of DS. The rationale between SC and DS is explained as follows. In a grid  $l$ , a relatively small  $DS_l$  indicates that grid  $l$  is oversupplied, and a relatively large  $DS_l$  means the grid is undersupplied. The goal of the platform is to get each  $DS_l$  as close to 1 as possible, meaning a balance between demand and supply. In a grid  $l$  with  $DS_l$  below 1,  $SC_l$  is expected to be large to discourage drivers from oversupplying the grid; while in a grid  $l$  with  $DS_l$  above 1,  $SC_l$  is supposed to be small. To demonstrate the rationale, we use a piecewise linear function with a parameter  $\alpha$  as SC in grid  $l$ , i.e.,

$$SC_l = \begin{cases} \alpha \times (1 - DS_l) & \text{if } DS_l \leq 1, \\ 0 & \text{otherwise,} \end{cases} \quad (12)$$

where a relatively high SC is applied to grids with a low DS and no SC is applied to grids with DS above 1.

With an adjustable parameter  $\alpha$ , the platform aims to maximize some objective  $f$ , consisting of two components, namely ORR and overall service charge (OSC), where

$$OSC = \frac{\sum_l \sum_{\text{order} \in l} SC_l \times \text{fare}_{\text{order}}}{\sum_l \sum_{\text{order} \in l} \text{fare}_{\text{order}}}.$$

The rationale of choosing these two components is as follows. First, from the perspective of the platform, it aims to maximize ORR, because a larger ORR typically means a higher revenue and a higher customer satisfaction. To maximize ORR, the platform simply chooses the largest possible value of  $\alpha$ . The reason is that with the largest possible  $\alpha$ , the platform penalizes drivers heavily for oversupplying a grid, and therefore drivers will be directed to other grids. This strategy, i.e., choosing the largest  $\alpha$ , however, is a big threat for the long-term growth of the platform because drivers are very likely to quit under such a high service charge. Thus, the platform also needs to maintain a relatively small OSC. Considering the competition between ORR and OSC, we use a weighted average of ORR and  $(1 - OSC)$  as the objective of the platform, i.e.,

$$f = w \times \text{ORR} + (1 - w) \times (1 - \text{OSC}), \quad (13)$$

where  $w \in [0, 1]$  is the weight for ORR. In this case study, we set  $w = \frac{3}{5}$ , meaning that the platform cares more about ORR. We then use two methods, namely, BO and an analytical method, to determine the optimal value of  $\alpha$ .

1. **BO.** We first employ BO with the objective function given in Equation (13). For a bilevel optimization problem, first we need to check the convergence of the lower level. As an example to validate the convergence, ORR and  $(1 - OSC)$  versus the index of iterations are presented in Figure (8) with  $\alpha = 0.6$ . ORR increases very fast and  $(1 - OSC)$  steadily decreases during the first 1,000 iterations where agents explore the environment and learn the optimal policy. ORR and  $(1 - OSC)$  gradually converge after 1,000 iterations when agents mainly exploit the knowledge they have gained through their previous explorations.

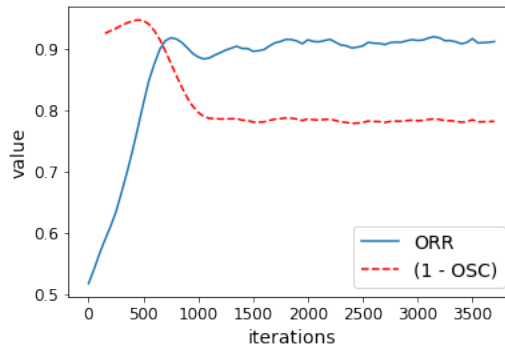


Figure 8: Convergence

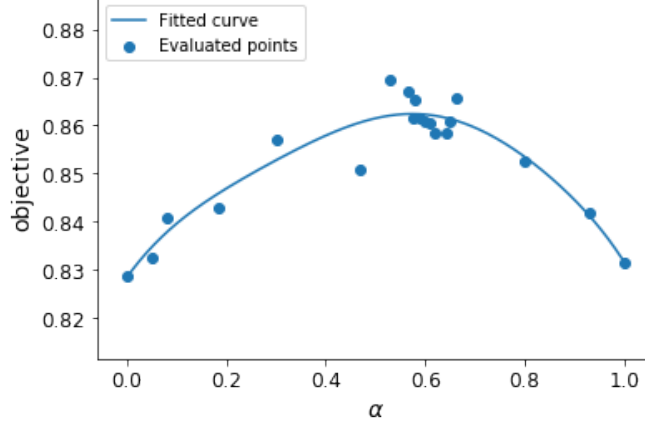


Figure 9: BO result

With the validated convergence of the lower level MAS, we run BO with a limited computation budget of 20 evaluations (i.e., we are only allowed to evaluate the objective at 20 different values of  $\alpha$ ). The result from BO is presented in Figure (9). It is noticeable that the evaluation of the objective on  $\alpha$ s seems quite noisy. In other words, the evaluated objective may be slightly different even for the same  $\alpha$ . This is expected because there are multiple local optima when solving the lower level MAS. Actually, it is commonly impossible to find a global optimum using deep learning, and researchers usually settle for local optima (Goodfellow et al., 2016). Local optima introduce noise into the evaluation of the objective at each  $\alpha$ . Although the evaluations are noisy, the fitted curve is able to capture the mean objective  $f$  for each  $\alpha$ . Due to a relatively flat shape of  $f$  around  $\alpha = 0.58$ , there are multiple  $\alpha$ s, i.e.,  $[0.51, 0.64]$ , yielding the same optimal mean objective, i.e., 0.862, which is 4.0% higher than the objective  $f = 0.829$  without any reward design.

2. **Analytical method.** Due to the simplicity of this case, we can analytically derive the optimal value of  $\alpha$  and shed some light on the effectiveness of the proposed platform service charge. Recall that the optimal policy for all drivers is to enter grid #4 when  $\alpha = 0$ . The resulting DS ratio in grid #4 is  $5/10 = 0.5$ , which is well below 1, meaning that grid #4 is oversupplied. ORR is  $5/7 = 71.43\%$ . To increase ORR, one needs to increase  $\alpha$  to penalize drivers who oversupply a grid. As  $\alpha$  gradually increases, grid #4 becomes less attractive, because the expected return one driver can earn decreases as  $\alpha$  increases. When the expected return one driver can earn is less than \$4.9, one driver will enter grid #1 instead of grid #4 for a higher monetary return. Note that to ease the analysis, we assume the number of drivers entering a grid is always an integer. Similarly, as one keeps increasing  $\alpha$ , the second driver will choose to enter #1 instead of grid #4. Now we present how we calculate the critical value of  $\alpha$  below which there is no driver choosing to enter grid #1 while above which there is one driver attracted by grid #1. With one driver entering grid #1, there are 9 drivers entering grid #4, resulting a  $5/9 = 0.556$  DS ratio in grid #4.  $SC_{\#4} = \alpha \times (1 - 0.556) = 0.444\alpha$ , meaning that the expected return for these 9 drivers is  $\frac{\$10 \times (1 - 0.444\alpha) \times 5}{9} = 5.556 \times (1 - 0.444\alpha)$ . The expected return for the driver entering grid #1 is \$4.9. We then have the critical condition  $5.556 \times (1 - 0.444\alpha) = 4.9$ , yielding  $\alpha = 0.266$ . Similarly, we can calculate the critical value of  $\alpha$  below which there is one driver choosing to enter grid #1 while above which there are two drivers attracted by grid #1, and the critical value is  $\alpha = 0.576$ .

Table 2: Values of interest

$\alpha$	0	0.266	0.576 (optimal)
DS ratio in grid #4	$5/10 = 50\%$	$5/9 = 55.6\%$	$5/8 = 62.5\%$
ORR	$5/7 = 71.43\%$	$6/7 = 85.71\%$	100%
OSC	0	0.107	0.181
$f$	0.829	0.871	0.928 (optimum)

Values of interest are presented in Table (2). With  $\alpha = 0$ ,  $\text{ORR} = 71.43\%$  and  $\text{OSC} = 0$ . The objective is  $\frac{3}{5} \times \text{ORR} + \frac{2}{5}(1 - \text{OSC}) = 0.829$ . With  $\alpha$  increasing to 0.266, there is one driver attracted by grid #1, resulting in a 85.71% ORR. The OSC is calculated as follows. The DS ratio in grid #4 is now 0.556, resulting in  $SC_{\#4} = 0.266 \times (1 - 0.556) = 0.118$ . Thus,  $\text{OSC} = \frac{\$10 \times 5 \times 0.118}{\$10 \times 5 + \$4.9} = 0.107$ . The objective is  $\frac{3}{5} \times \text{ORR} + \frac{2}{5}(1 - \text{OSC}) = 0.871$ . Similarly, with  $\alpha$  increasing to 0.576,  $\text{ORR} = 100\%$ ,  $\text{OSC} = 0.181$ , and the objective is 0.928. Increasing  $\alpha$  further does not improve ORR but increases OSC, resulting in a decrease in the objective. Thus, the analytically derived optimal value of  $\alpha$  is 0.576.

The analytically derived optimal value of  $\alpha$ , i.e., 0.576, agrees well with the derived optimal range of  $\alpha$  from BO, i.e.,  $[0.51, 0.64]$ . The optimum from the analytical solution, i.e., 0.928, however, deviates from its numerical counterpart, i.e., 0.862. The reason is explained as follows. First, in the analytical solution, the policy for agents is deterministic and exact two drivers choose grid #1 after increasing  $\alpha$  to 0.576; while in BO, the derived optimal policy for agents with is stochastic, introducing variance in drivers' actions. For example, each driver has a 20% probability of choosing grid #1 and a 80% probability of choosing grid #4. Although the expected number of agents in grid #1 is 2 and the expected number of agents in grid #4 is 8, the probability of all agents choosing grid #4 is  $0.8^{10} = 10.7\%$ . This variance reduces both ORR and  $(1 - \text{OSC})$ , resulting in a lower objective from BO, compared with the objective from the analytical solution. Second, for a given  $\alpha$ , there are multiple local optima when solving the lower level MAS, which may also contribute to a smaller objective.

Despite the intrinsic difference in the policy between the analytical approach and the numerical method (i.e., BO), the overall agreement in the optimal value of  $\alpha$  from both methods validates the proposed bilevel optimization model. Although the derived optimal  $\alpha \in [0.51, 0.64]$  seems large, it represents the service charge at a DS ratio of zero and DS ratio typically does not go below some value (e.g., 0.5 in this case). Actually, the OSC is 0.181 which falls in a reasonable range. It is also worth mentioning that the objective can be increased by 4.0% using a simple platform service charge. Other forms of reward design may better improve the performance of the platform and are left in future research.

## 6. Conclusion

Noticing the underutilization of taxi resources due to idle taxi drivers' cruising behavior, this study aims to model the multi-driver repositioning task through a mean field multi-agent reinforcement learning approach. A mean field actor-critic algorithm is developed to solve the MAS with a given reward function. The direct application of the mean field actor-critic algorithm to the MAS is, however, very likely to yield a suboptimal equilibrium from the standpoint of the system. Thus, this study proposes a bilevel optimization with the upper level as a reward design and the lower level as the MAS. The upper level interacts with the lower level by adjusting the reward for the MAS.

To improve the performance of the system, current studies intentionally craft a reward function which aligns with the goal of the system but may not reflect the intrinsic reward of real drivers. In other words, drivers are forced to cooperate, which is not the real case. In this study, we treat drivers as selfish and non-cooperative. Drivers aim to maximize their own interests instead of the performance of the system. The central controller (e.g., the e-hailing platform) achieves its goal by adjusting the reward that a driver can earn. To effectively solve the optimal control parameter, we adopted a Bayesian optimization approach.

The bilevel optimization model is applied a synthetic dataset. Using a simple piecewise linear platform service charge, the optimal intercept is derived as a range of  $[0.51, 0.64]$ . The results show that the objective of the platform can be improved by 4% using the proposed simple platform service charge, compared with no reward design. More complicated forms of reward design are believed to better increase the performance of the platform and are left in future research.

## References

- Brown, N., Sandholm, T., Jan. 2018. Superhuman AI for heads-up no-limit poker: Libratus beats top professionals. *Science* 359 (6374), 418–424.
- Brown, N., Sandholm, T., Aug. 2019. Superhuman AI for multiplayer poker. *Science* 365 (6456), 885–890.



- Buoniu, L., Babuka, R., De Schutter, B., 2010. Multi-agent Reinforcement Learning: An Overview. In: Srinivasan, D., Jain, L. C. (Eds.), *Innovations in Multi-Agent Systems and Applications - 1. Studies in Computational Intelligence*. Springer Berlin Heidelberg, Berlin, Heidelberg, pp. 183–221.
- Foerster, J. N., Assael, Y. M., de Freitas, N., Whiteson, S., 2016. Learning to Communicate with Deep Multi-agent Reinforcement Learning. In: *Proceedings of the 30th International Conference on Neural Information Processing Systems. NIPS'16*. Curran Associates Inc., USA, pp. 2145–2153, event-place: Barcelona, Spain.
- Frazier, P. I., Jul. 2018. A Tutorial on Bayesian Optimization. arXiv:1807.02811 [cs, math, stat]ArXiv: 1807.02811.
- Gao, Y., Jiang, D., Xu, Y., Aug. 2018. Optimize taxi driving strategies based on reinforcement learning. *International Journal of Geographical Information Science* 32 (8), 1677–1696.
- Ge, Y., Xiong, H., Tuzhilin, A., Xiao, K., Gruteser, M., Pazzani, M., 2010. An Energy-efficient Mobile Recommender System. In: *Proceedings of the 16th ACM SIGKDD International Conference on Knowledge Discovery and Data Mining. KDD '10*. ACM, New York, NY, USA, pp. 899–908.
- Goodfellow, I., Bengio, Y., Courville, A., 2016. *Deep Learning*. MIT Press, <http://www.deeplearningbook.org>.
- Grondman, I., Busoniu, L., Lopes, G. A. D., Babuska, R., Nov. 2012. A Survey of Actor-Critic Reinforcement Learning: Standard and Natural Policy Gradients. *IEEE Transactions on Systems, Man, and Cybernetics, Part C (Applications and Reviews)* 42 (6), 1291–1307.
- Hwang, R.-H., Hsueh, Y.-L., Chen, Y.-T., Sep. 2015. An effective taxi recommender system based on a spatio-temporal factor analysis model. *Information Sciences* 314, 28–40.
- Jin, J., Zhou, M., Zhang, W., Li, M., Guo, Z., Qin, Z., Jiao, Y., Tang, X., Wang, C., Wang, J., Wu, G., Ye, J., 2019. CoRide: Joint Order Dispatching and Fleet Management for Multi-Scale Ride-Hailing Platforms. In: *Proceedings of the 28th ACM International Conference on Information and Knowledge Management. CIKM '19*. ACM, New York, NY, USA, pp. 1983–1992, event-place: Beijing, China.
- Konda, V. R., Tsitsiklis, J. N., Apr. 2003. On Actor-Critic Algorithms. *SIAM J. Control Optim.* 42 (4), 1143–1166.
- Li, M., Qin, Z., Jiao, Y., Yang, Y., Wang, J., Wang, C., Wu, G., Ye, J., 2019. Efficient Ridesharing Order Dispatching with Mean Field Multi-Agent Reinforcement Learning. In: *The World Wide Web Conference. WWW '19*. ACM, New York, NY, USA, pp. 983–994, event-place: San Francisco, CA, USA.
- Lin, K., Zhao, R., Xu, Z., Zhou, J., 2018. Efficient Large-Scale Fleet Management via Multi-Agent Deep Reinforcement Learning. In: *Proceedings of the 24th ACM SIGKDD International Conference on Knowledge Discovery & Data Mining. KDD '18*. ACM, New York, NY, USA, pp. 1774–1783.
- Littman, M. L., 1994. Markov Games As a Framework for Multi-agent Reinforcement Learning. In: *Proceedings of the Eleventh International Conference on International Conference on Machine Learning. ICML'94*. Morgan Kaufmann Publishers Inc., San Francisco, CA, USA, pp. 157–163, event-place: New Brunswick, NJ, USA.
- Lowe, R., Wu, Y., Tamar, A., Harb, J., Abbeel, P., Mordatch, I., 2017. Multi-agent Actor-critic for Mixed Cooperative-competitive Environments. In: *Proceedings of the 31st International Conference on Neural Information Processing Systems. NIPS'17*. Curran Associates Inc., USA, pp. 6382–6393, event-place: Long Beach, California, USA.
- Matignon, L., Laurent, G. J., Fort-Piat, N. L., Feb. 2012. Independent reinforcement learners in cooperative Markov games: a survey regarding coordination problems. *The Knowledge Engineering Review* 27 (1), 1–31.
- Mguni, D., Jennings, J., Macua, S. V., Sison, E., Ceppi, S., Cote, E. M. d., 2018. Coordinating the Crowd: Inducing Desirable Equilibria in Non-Cooperative Systems. In: *NeurIPS Workshop on Machine Learning for Intelligent Transportation Systems*.
- Mnih, V., Kavukcuoglu, K., Silver, D., Rusu, A. A., Veness, J., Bellemare, M. G., Graves, A., Riedmiller, M., Fidjeland, A. K., Ostrovski, G., Petersen, S., Beattie, C., Sadik, A., Antonoglou, I., King, H., Kumaran, D., Wierstra, D., Legg, S., Hassabis, D., Feb. 2015. Human-level control through deep reinforcement learning. *Nature* 518 (7540), 529–533.
- Nguyen, T. T., Nguyen, N. D., Nahavandi, S., Dec. 2018. Deep Reinforcement Learning for Multi-Agent Systems: A Review of Challenges, Solutions and Applications. arXiv:1812.11794 [cs, stat]ArXiv: 1812.11794.
- OpenAI, 2018. Openai five. <https://blog.openai.com/openai-five/>.
- Powell, J. W., Huang, Y., Bastani, F., Ji, M., 2011. Towards Reducing Taxicab Cruising Time Using Spatio-temporal Profitability Maps. In: *Proceedings of the 12th International Conference on Advances in Spatial and Temporal Databases. SSTD'11*. Springer-Verlag, Berlin, Heidelberg, pp. 242–260.
- Puterman, M. L., 1994. *Markov Decision Processes: Discrete Stochastic Dynamic Programming*, 1st Edition. John Wiley & Sons, Inc., New York, NY, USA.
- Qu, M., Zhu, H., Liu, J., Liu, G., Xiong, H., 2014. A Cost-effective Recommender System for Taxi Drivers. In: *Proceedings of the 20th ACM SIGKDD International Conference on Knowledge Discovery and Data Mining. KDD '14*. ACM, New York, NY, USA, pp. 45–54.
- Rong, H., Zhou, X., Yang, C., Shafiq, Z., Liu, A., 2016. The Rich and the Poor: A Markov Decision Process Approach to Optimizing Taxi Driver Revenue Efficiency. In: *Proceedings of the 25th ACM International Conference on Information and Knowledge Management. CIKM '16*. ACM, New York, NY, USA, pp. 2329–2334.
- Shou, Z., Di, X., Ye, J., Zhu, H., Zhang, H., Hampshire, R., Feb. 2020. Optimal passenger-seeking policies on E-hailing platforms using Markov decision process and imitation learning. *Transportation Research Part C: Emerging Technologies* 111, 91–113.
- Silver, D., Huang, A., Maddison, C. J., Guez, A., Sifre, L., van den Driessche, G., Schrittwieser, J., Antonoglou, I., Panneershelvam, V., Lanctot, M., Dieleman, S., Grewe, D., Nham, J., Kalchbrenner, N., Sutskever, I., Lillicrap, T., Leach, M., Kavukcuoglu, K., Graepel, T., Hassabis, D., Jan. 2016. Mastering the game of Go with deep neural networks and tree search. *Nature* 529 (7587), 484–489.
- Silver, D., Schrittwieser, J., Simonyan, K., Antonoglou, I., Huang, A., Guez, A., Hubert, T., Baker, L., Lai, M., Bolton, A., Chen, Y., Lillicrap, T., Hui, F., Sifre, L., van den Driessche, G., Graepel, T., Hassabis, D., Oct. 2017. Mastering the game of Go without human knowledge. *Nature* 550 (7676), 354–359.
- Sutton, R. S., Barto, A. G., 1998. *Introduction to Reinforcement Learning*, 1st Edition. MIT Press, Cambridge, MA, USA.
- Sutton, R. S., McAllester, D., Singh, S., Mansour, Y., 1999. Policy Gradient Methods for Reinforcement Learning with Function Approximation. In: *Proceedings of the 12th International Conference on Neural Information Processing Systems. NIPS'99*. MIT Press, Cambridge, MA, USA, pp. 1057–1063, event-place: Denver, CO.

- Tampuu, A., Matiisen, T., Kodelja, D., Kuzovkin, I., Korjus, K., Aru, J., Aru, J., Vicente, R., Apr. 2017. Multiagent cooperation and competition with deep reinforcement learning. *PLOS ONE* 12 (4), e0172395.
- Tan, M., 1993. Multi-Agent Reinforcement Learning: Independent vs. Cooperative Agents. In: *Proceedings of the Tenth International Conference on Machine Learning*. Morgan Kaufmann, pp. 330–337.
- Verma, T., Varakantham, P., Kraus, S., Lau, H. C., Jun. 2017. Augmenting decisions of taxi drivers through reinforcement learning for improving revenues. *Proceedings of the Twenty-Seventh International Conference on Automated Planning and Scheduling ICAPS 2017: Pittsburgh, June 18-23*, 409–417.
- Vinyals, O., Babuschkin, I., Czarnecki, W. M., Mathieu, M., Dudzik, A., Chung, J., Choi, D. H., Powell, R., Ewalds, T., Georgiev, P., Oh, J., Horgan, D., Kroiss, M., Danihelka, I., Huang, A., Sifre, L., Cai, T., Agapiou, J. P., Jaderberg, M., Vezhnevets, A. S., Leblond, R., Pohlen, T., Dalibard, V., Budden, D., Sulsky, Y., Molloy, J., Paine, T. L., Gulcehre, C., Wang, Z., Pfaff, T., Wu, Y., Ring, R., Yogatama, D., Wnsch, D., McKinney, K., Smith, O., Schaul, T., Lillicrap, T., Kavukcuoglu, K., Hassabis, D., Apps, C., Silver, D., Nov. 2019. Grandmaster level in StarCraft II using multi-agent reinforcement learning. *Nature* 575 (7782), 350–354.
- Yang, Y., Luo, R., Li, M., Zhou, M., Zhang, W., Wang, J., Jul. 2018. Mean Field Multi-Agent Reinforcement Learning. In: *International Conference on Machine Learning*. pp. 5571–5580.
- Yu, X., Gao, S., Hu, X., Park, H., Mar. 2019. A Markov decision process approach to vacant taxi routing with e-hailing. *Transportation Research Part B: Methodological* 121, 114–134.
- Yuan, J., Zheng, Y., Zhang, L., Xie, X., Sun, G., 2011. Where to Find My Next Passenger. In: *Proceedings of the 13th International Conference on Ubiquitous Computing. UbiComp '11*. ACM, New York, NY, USA, pp. 109–118.
- Zhang, K., Yang, Z., Baar, T., Nov. 2019. Multi-Agent Reinforcement Learning: A Selective Overview of Theories and Algorithms. URL <https://arxiv.org/abs/1911.10635v1>
- Zhou, M., Jin, J., Zhang, W., Qin, Z., Jiao, Y., Wang, C., Wu, G., Yu, Y., Ye, J., 2019. Multi-Agent Reinforcement Learning for Order-dispatching via Order-Vehicle Distribution Matching. In: *Proceedings of the 28th ACM International Conference on Information and Knowledge Management. CIKM '19*. ACM, New York, NY, USA, pp. 2645–2653, event-place: Beijing, China.
- Zhou, X., Rong, H., Yang, C., Zhang, Q., Khezerlou, A. V., Zheng, H., Shafiq, M. Z., Liu, A. X., 2018. Optimizing Taxi Driver Profit Efficiency: A Spatial Network-based Markov Decision Process Approach. *IEEE Transactions on Big Data*, 1–1.